THE JOURNAL OF BIOLOGICAL CHEMISTRY VOL. 284, NO. 14, pp. 9521–9528, April 3, 2009

Mammalian Heat Shock Factor 1 Is Essential for Oocyte Meiosis and Directly Regulates Hsp90α Expression*[S]

Received for publication, November 20, 2008, and in revised form, January 20, 2009 Published, JBC Papers in Press, January 21, 2009, DOI 10.1074/jbc.M808819200

Aïcha Metchat[‡], Malin Åkerfelt[§1], Christiane Bierkamp[‡], Virginie Delsinne[¶], Lea Sistonen[§], Henri Alexandre[¶], and Elisabeth S. Christians[‡2]

From [‡]UPS, Centre de Biologie du Développement-UMR5547, 4R3B3, Université de Toulouse, 118 route de Narbonne, F-31062 Toulouse, France, [§]Department of Biology, Åbo Akademi University, Turku Centre for Biotechnology, University of Turku, Åbo Akademi University, 20520 Turku, Finland, and [¶]Département de Biologie, Université de Mons-Hainaut, Faculté de Médecine-Pharmacie, 7000 Mons, Belgium

Heat shock transcription factor 1 (HSF1) is the main regulator of the stress response that triggers the transcription of several genes encoding heat shock proteins (Hsps). Hsps act as molecular chaperones involved in protein folding, stability, and trafficking. HSF1 is highly expressed in oocytes and *Hsf1* knock-out in mice revealed that in the absence of stress this factor plays an important role in female reproduction. We previously reported that *Hsf1*$^{-/-}$ females produce oocytes but no viable embryos. Consequently, we asked whether oocytes require HSF1 to regulate a particular set of Hsps necessary for them to develop. We find that Hsp90α (Hspaa1) is the major HSF1-dependent chaperone inasmuch as *Hsf1* knock-out resulted in Hsp90-depleted oocytes. These oocytes exhibited delayed germinal vesicle breakdown (or G_2/M transition), partial meiosis I block, and defective asymmetrical division. To probe the role of Hsp90α in this meiotic syndrome, we analyzed meiotic maturation in wild-type oocytes treated with a specific inhibitor of Hsp90, 17-allylamino-17-demethoxy-geldanamycin, and observed similar defects. At the molecular level we showed that, together with these developmental anomalies, CDK1 and MAPK, key meiotic kinases, were significantly disturbed. Thus, our data demonstrate that HSF1 is a maternal transcription factor essential for normal progression of meiosis.

In mammals there are several heat shock factors (HSF1, -2, and -4)[3] that share a similar DNA binding domain, but HSF1 appears to be the major transcriptional regulator responsible for the stress-inducible expression of heat shock proteins (Hsps) (1, 2). The *Hsf1* gene was targeted by homologous recombination in murine ES cells, and *Hsf1* knock-out mice were produced by three different laboratories (3–5). Gene expression analyses in various cell types, and organs derived from these *Hsf1*$^{-/-}$ mice revealed that HSF1 also regulates Hsp in physiological conditions (6–8), providing accumulating evidence for the important function of HSF1 in maintaining cell homeostasis. Furthermore, those analyses and genome-wide screen demonstrated that numerous genes that were not classified as Hsps appeared to be HSF1-dependent (8, 9). Thus, HSF1 is clearly not restricted to the control of Hsp expression or the heat shock response. As shown by the complex phenotype of *Hsf1* knock-out mice, HSF1 is involved in several specialized cell functions (*e.g.* placenta formation, immunity, placode development, cancer cell viability) (3, 5, 10, 11) and is essential for female reproduction (3). We showed previously that *Hsf1*$^{-/-}$ female infertility is linked to the inability of *Hsf1*$^{-/-}$ oocytes to produce viable embryos after natural mating (12). Nevertheless, the molecular and cellular mechanisms affected by the loss of HSF1 function in oocytes required further investigation to be better understood.

Because HSF1 is highly expressed in oocytes, we hypothesized that it could regulate critical Hsps for the final development of oocytes into embryos. Although a series of studies separately analyzed several Hsps in rodent oocytes (see the references in Christians *et al.* (2) and more recently for Hsp105, (13)), no comprehensive picture of the expression and regulation of maternal Hsps emerged. Furthermore, Hsps are likely to be important maternal proteins because they act as chaperones, transiently interacting with other proteins (named clients for Hsp90 interacting candidates) to support numerous cellular processes ranging from cytoskeleton assembly to cell cycle control (14). However, the limited number of *Hsp* gene knockouts (Hsp25, Hsp70.1-Hsp70.3, Hsp90β) has not yet revealed the functional importance of any Hsp in oocytes either because there was no effect due to redundancy of Hsp function (15–17) or because the appearance of lethal phenotypes did not allow the appropriate analysis (*e.g.* Hsp90β knockouts died around 10 days post-coitus (18)).

* This work was funded by the Centre National de la Recherche Scientifique, le Ministère de l'Education Nationale et de la Recherche, la Fondation pour la Recherche Médicale (to E. S. C.), l'Association pour la Recherche contre le Cancer (to A. M.), travel grants funding from the University Toulouse III (UPS) (to A. M. and E. S. C.), and by The Academy of Finland, The Sigrid Jusélius Foundation, and Åbo Akademi University (to L. S.). The costs of publication of this article were defrayed in part by the payment of page charges. This article must therefore be hereby marked "*advertisement*" in accordance with 18 U.S.C. Section 1734 solely to indicate this fact.

[S] The on-line version of this article (available at http://www.jbc.org) contains supplemental Tables S1–S3 and Figs. 1 and 2.

[1] Supported by the Turku Graduate School of Biochemical Sciences.

[2] To whom correspondence should be addressed. Fax: 33-561-55-6507; E-mail: Elisabeth.Christians@cict.fr.

[3] The abbreviations used are: HSF, heat shock factor; Hsp, heat shock protein; ChIP, chromatin immunoprecipitation; MII, metaphase II; GVBD, germinal vesicle (GV) breakdown; 17AAG, 17-(allylamino)-17-demethoxygelda-namycin; MEK, mitogen-activated protein kinase/extracellular signal-regulated kinase kinase; IBMX, isobutylmethylxanthine; ERK, extracellular signal-regulated kinase; MAPK, mitogen-activated protein (MAP) kinase; ERK1/2-P, ERK1/2 phosphorylated forms; qPCR, quantitative PCR.

Here we show that HSF1 differentially regulates Hsps and is required for the accumulation of large amounts of Hsp90α in fully grown oocytes. We provide evidence that both Hsp90-depleted (*Hsf1*$^{-/-}$) and Hsp90-inhibited (17-(allylamino)-17-demethoxygelda-namycin (17AAG)-treated *Hsf1*$^{+/+}$) oocytes suffer from a series of similar anomalies that impair meiosis progression, an obligatory step to prepare eggs for fertilization. This strongly suggests that Hsp90α deficit significantly contributes to the developmental defects seen in *Hsf1*$^{-/-}$ oocytes. Together, our data identify HSF1 as a new meiotic factor in mammals.

EXPERIMENTAL PROCEDURES

Mice—Hsf1$^{+/+}$ and *Hsf1*$^{-/-}$ mice, a gift from Dr. I. J. Benjamin (Salt Lake City, UT), have been described elsewhere (19). They were maintained in a mixed genetic background. Protocols for animal breeding and experiments were approved by the Departmental Veterinary Office (Haute-Garonne) according to French legislation.

Oocyte Collection and Culture—Hsf1$^{+/+}$ and *Hsf1*$^{-/-}$ oocytes were collected and cultured according to previously described procedures (20). Media (M2, M16, Sigma) were supplemented as indicated with IBMX (45 μg/ml, 1000× in DMSO, Sigma), 17AAG (1.78 μM, stock solution 1000× in DMSO, Sigma) (21), or cycloheximide (20 μg/ml, stock 2000× in ethanol).

Real-time Reverse Transcription Quantitative PCR Analysis—Oocyte samples stored at −80 °C (20 oocytes) were thawed and mixed with up to 2 μl of lysis buffer (0.8% IGEPAL, (Sigma), 1 unit/μl RNasin, 5 mM dithiothreitol). Before reverse transcription, samples were heated at 75 °C for 5 min and transferred immediately to ice. DNase treatment was performed by adding 3 μl of DNA lysis buffer (2.5 mM $MgCl_2$, 5× buffer (Invitrogen), 30 units of DNase I-RNase-free (Roche Applied Science) to the sample followed by incubation for 1 h at 25 °C and 5 min at 70 °C. The reverse transcription reaction was carried out according to the manufacturer's instructions. The samples were subjected to oligonucleotide (dT)-primed first-strand cDNA synthesis in a final volume of 20 μl using the SuperScriptII reverse transcriptase kit (Invitrogen). cDNA was synthesized at 42 °C for 1.5 h. The qPCR reaction was performed on an iCycler device (Bio-Rad) using Platinum SYBR Green qPCR Super-Mix-UDG (Invitrogen) according to the manufacturer's instructions. Primer sequences are listed in supplemental Table S1. Each reaction was performed in triplicate with an amount of cDNA corresponding to a single oocyte. Ribosomal protein S16 (S16) cDNA was used as an internal control to normalize the data, which were analyzed with the $2^{-\Delta\Delta CT}$ method (22).

Chromatin Immunoprecipitation (ChIP)—The ChIP protocol was modified from Chang *et al.* (23). Five ovaries were lysed in 3 ml of lysis buffer. Antibodies and primer sequences are listed in supplemental Tables S1 and S2.

Western Blot Analysis—Fully grown oocytes stored at −80 °C were thawed, supplemented with sample buffer (24), and heated to 100 °C for 5 min, and total protein extracts were then subjected to one-dimensional SDS-PAGE followed by transfer on to nitrocellulose membranes. Blots were incubated in blocking buffer (Tris-buffered saline (TBS) containing 1% Tween 20 (TBS-T) and 5% milk) overnight at 4 °C and then incubated with the primary antibody in TBS containing 2–3% milk, 0.2% Tween 20) for 2 h at room temperature. Antibodies are listed in supplemental Table S2. The membranes were washed 3 times in TBS-T and then incubated in TBS-T, 2% milk to which appropriate horseradish peroxidase-conjugated secondary antibody was added. After several washes, membranes were developed with an enhanced chemiluminescence method (SuperSignal West Pico Chemiluminescent Substrate, Pierce).

Immunostaining of Oocytes and Ovary Sections—Mouse oocytes were immunostained following the procedure described elsewhere (20) and analyzed with a Leica TCS SP-5 spectral confocal (Plateforme Toulouse RIO-Imaging, CBD-IFR109). For immunohistochemistry, mouse ovaries were fixed with Bouin, and histological preparations were performed according to a classical procedure (Plateau Technique d'Histopathologie Expérimentale de l'IFR30, Plateforme d'Exploration fonctionnelle/Génopole, Toulouse Midi-Pyrénées). Immunohistochemistry was performed according to a previously described procedure (25). Antibodies are described in supplemental Table S2.

Imaging Analysis—A confocal microscope (Leica Microsystems, Heidelberg GmbH, Microscope confocal Leica SP5) was used for monitoring spindles and chromosomes in the immunolocalization experiments. An HCX PL APO 40.0×/1.25 NA oil immersion lens was used at room temperature. For fluorescein isothiocyanate, an argon laser was used with a 488-nm laser line and emission between 500- and 600-nm spectral detection range. The 543-nm laser line of a helium-neon laser provided excitation of Alexa Fluor 546, and fluorescence was collected using a 555–631-nm spectral detection range. For imaging TO-PRO-3, confocal images were obtained by exciting with the 633-nm laser line of a HeNe laser, and emission was collected through a 650–750-nm spectral detection range. For all confocal imaging experiments, a pinhole of 1 Airy unit was used.

RESULTS

HSF1 Differentially Regulates Hsp Expression in Oocytes—Using reverse transcription followed by real-time PCR (qPCR), we examined mRNA levels of the major members of several Hsp families: Hsp25, Hsp60, Hsp70.1, Hsp70.3, Hsp90α, Hsp90β, Hsp105 (see gene descriptions in supplemental Table S1). These experiments revealed that Hsp90α transcripts were the most abundant in fully grown *Hsf1*$^{+/+}$ oocytes. The levels of Hsp90β and Hsp105 transcripts were approximately one-fourth that of Hsp90α, whereas the transcripts of Hsp25, Hsp60, and Hsp70.1 were 100-fold less abundant, and Hsp70.3 transcripts were hardly detectable (Fig. 1*A*). Compared with *Hsf1*$^{+/+}$, *Hsf1*$^{-/-}$ oocytes were markedly depleted in Hsp90α and exhibited visible down-regulation for Hsp70.1 and Hsp25 transcripts, but there was no difference for Hsp60 or Hsp90β transcripts (Fig. 1*B*). The effect of HSF1 deficiency on Hsp70.3 expression could not be determined because of the very low signals obtained in *Hsf1*$^{+/+}$ and *Hsf1*$^{-/-}$ oocytes (Fig. 1, *A* and *B*).

To demonstrate that HSF1 is the direct transcriptional regulator of Hsp90α gene, we undertook ChIP experiments using

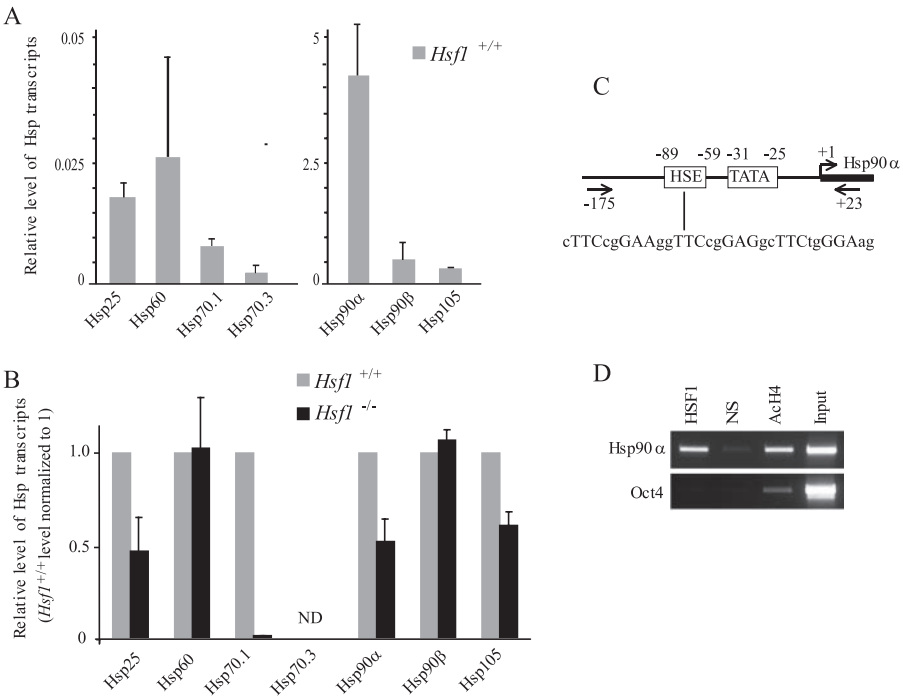

FIGURE 1. **Characterization of Hsp expression and regulation in fully grown oocytes.** *A*, relative RNA levels of seven Hsp genes (Hsp25, Hsp60, Hsp70.1, Hsp70.3, Hsp90α, Hsp90β, Hsp105) were measured by reverse transcription-qPCR in *Hsf1*$^{+/+}$ oocytes. The gene encoding the ribosomal protein S16 was used as an internal control to normalize the data. Two different *y* scales were used to adequately display the relative level of transcripts for each gene. *B*, relative RNA levels of the same seven Hsp genes were compared between *Hsf1*$^{+/+}$ and *Hsf1*$^{-/-}$ oocytes. Data are presented relative to the level obtained with *Hsf1*$^{+/+}$ oocytes. *ND* indicates that values could not be determined for Hsp70.3 transcripts. *A* and *B*, means ± S.D. *C*, schematic illustration of the proximal Hsp90α promoter region. *HSE* (heat shock element) is indicated with the sequence including the HSF1 binding site. TATA corresponds to the TATA-box and the transcription start site is shown as a *bent arrow* (45). *Arrows*, primers used in the ChIP assay. *D*, HSF1 ChIP. HSF1 binds the Hsp90α but not the Oct4 promoter in *Hsf1*$^{+/+}$ ovary. Nonspecific antibody (*NS*) was used as a negative control, and acetylated histone 4 antibody (*AcH4*) was used as an indicator of transcriptionally active promoters.

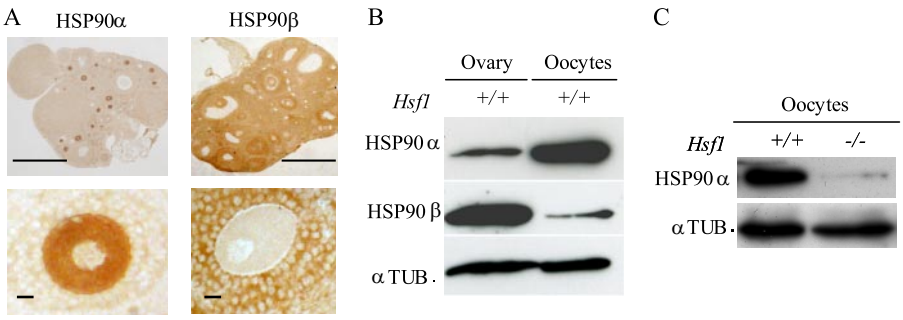

FIGURE 2. **Expression of Hsp90 cytoplasmic isoforms Hsp90α (Hsp90aa1) and β (Hsp90ab1).** *A*, histological sections of *Hsf1*$^{+/+}$ ovaries were immunostained with specific antibodies against Hsp90α and β (*upper panels*). Higher magnification of fully grown oocytes surrounded by granulosa cells revealed the differential localization of both Hsp90s; Hsp90α is concentrated in oocyte cytoplasm, and Hsp90β is found in granulosa cells. *Bars*, 1 mm (*upper panels*); 50 μm (*lower panels*). *B*, levels of Hsp90α and Hsp90β proteins analyzed by Western blot prepared with total extracts either from ovary (30 μg) or isolated oocytes (n = 100). *C*, level of Hsp90α in *Hsf1*$^{+/+}$ and *Hsf1*$^{-/-}$ oocytes (n = 40). *B* and *C*, tubulin (α*TUB.*) was used as the loading control.

scripts. We further characterized the corresponding protein and compared the two cytoplasmic Hsp90s, Hsp90α and -β. Histological sections showed that Hsp90α was concentrated in oocyte cytoplasm and Hsp90β in follicular cells (Fig. 2*A*). Western blots performed with protein extracts from ovary revealed the presence of Hsp90α and -β (Fig. 2*B*). Hsp90α was easily detected in a total protein extract from 100 oocytes (Fig. 2*B*, after a 1-min exposure of the membrane). In contrast, even after a longer exposure (30 min), only a weak signal was visible in the case of Hsp90β (Fig. 2*B*). Thus, murine oocytes appear different from most somatic cells in that expression of Hsp90α overwhelmingly predominates over that of Hsp90β. In accordance with the reduction of Hsp90α transcripts, the level of Hsp90α protein is markedly reduced in *Hsf1*$^{-/-}$ oocytes (Fig. 2*C*).

Disturbed Meiotic Progression in Hsf1$^{-/-}$ *Oocytes*—During development, oogonia enter meiosis at 13.5 days post-coitus, and oocytes remain blocked at prophase I until they are fully grown. Then, in response to hormonal signal or after experimental isolation from their ovarian follicles, oocytes resume meiosis, enter meiotic maturation, and progress to metaphase II (MII), at which stage they can be fertilized (Fig. 3*A*). Because fully grown *Hsf1*$^{-/-}$ oocytes do not exhibit morphological anomalies but are molecularly deficient in chaperones (this paper), we decided next to carefully examine these early developmental steps, which are essential prerequisites for obtaining normal embryos.

We analyzed by video time-lapse microscopy the meiotic maturation of oocytes cultured *in vitro*. Resumption of meiosis, characterized by the disappearance of the nucleus (also named germinal vesicle (GV) breakdown (GVBD)), was seen to be significantly retarded in *Hsf1*$^{-/-}$ oocytes. The transition GV-GVBD occurred on average after 69.5 ± 8.65 min for *Hsf1*$^{+/+}$ oocytes compared with 285 ± 26 min for *Hsf1*$^{-/-}$ oocytes (mean ± S.E. calculated from data presented in Fig. 3*B*, $p < 0.001$). Eventually, *Hsf1*$^{-/-}$ oocytes progressed through meiosis, but only 16.4% (n = 70/427) of

specific primers flanking HSF1 binding site (heat shock element (*HSE*)) located in Hsp90α promoter (Fig. 1*C*). We used total ovary extracts to obtain as much material as possible, as HSF1 was found to be specifically expressed in oocytes at all stages of ovarian oogenesis (supplemental Fig. S1). As shown in Fig. 1*D*, HSF1 bound the promoter of Hsp90α but not the regulatory region of Oct4, which is another gene that is highly active in oocytes. Taken together, these data indicate that HSF1 is required to store large amounts of Hsp90α tran-

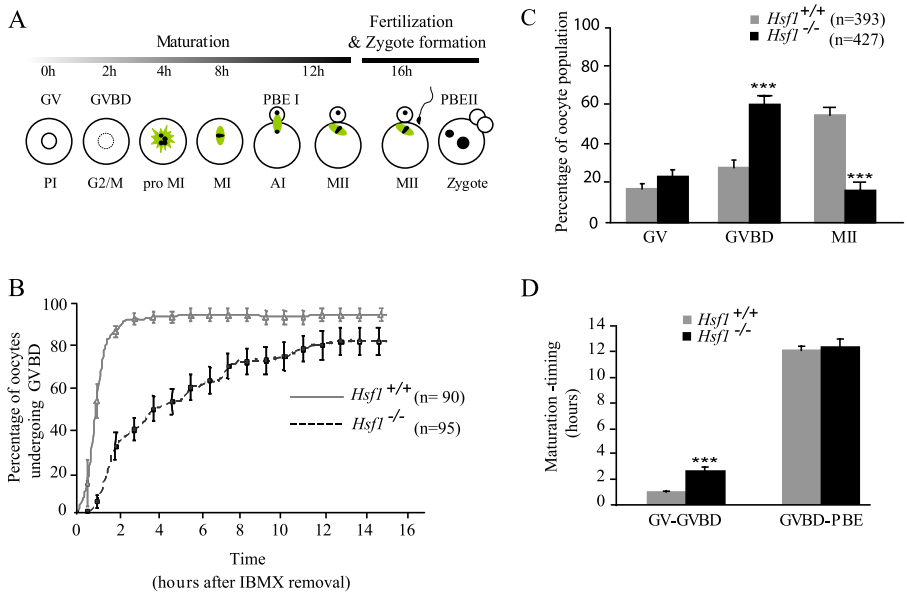

FIGURE 3. **Delay and blockage of meiotic maturation in *Hsf1*$^{-/-}$ oocytes.** *A*, meiosis is initiated during embryonic development, and oocytes remain arrested at the end of prophase I (*PI*). After hormonal signaling or isolation from ovaries, oocytes resume meiosis. The timing is indicated for the different meiotic stages from GV to GVBD, pro-metaphase I (*pro-MI*), metaphase I (*MI*), anaphase I (*AI*), cytokinesis, or polar body extrusion (*PBE*) and finally metaphase II (*MII*). Mature (*MII*) oocytes are ready to be fertilized and to undertake the second meiotic division before progressing to the first mitotic cell cycle (zygote). The main features of the microtubular cytoskeleton are schematized in *green*. *B*, GVBD in *Hsf1*$^{+/+}$ and *Hsf1*$^{-/-}$ oocytes after IMBX removal ($t = 0$ h) was analyzed by video time-lapse microscopy. The percentage of GVBD in *Hsf1*$^{+/+}$ and *Hsf1*$^{-/-}$ oocytes was plotted from 0 to 16 h after IBMX removal. *C*, maturation was evaluated in *Hsf1*$^{+/+}$ and *Hsf1*$^{-/-}$ oocytes after 16 h of culture. Oocytes were scored under the microscope according to their meiotic stage, either GV, GVBD (absence of GV), and MII (absence of GV and extruded first polar body-*PBE*). *D*, meiosis timing in oocytes that successfully achieved maturation was retrospectively measured for two main steps (transition from GV to GVBD and from GVBD to PBE). *B–D*, means ± S.E. ***, $p < 0.001$.

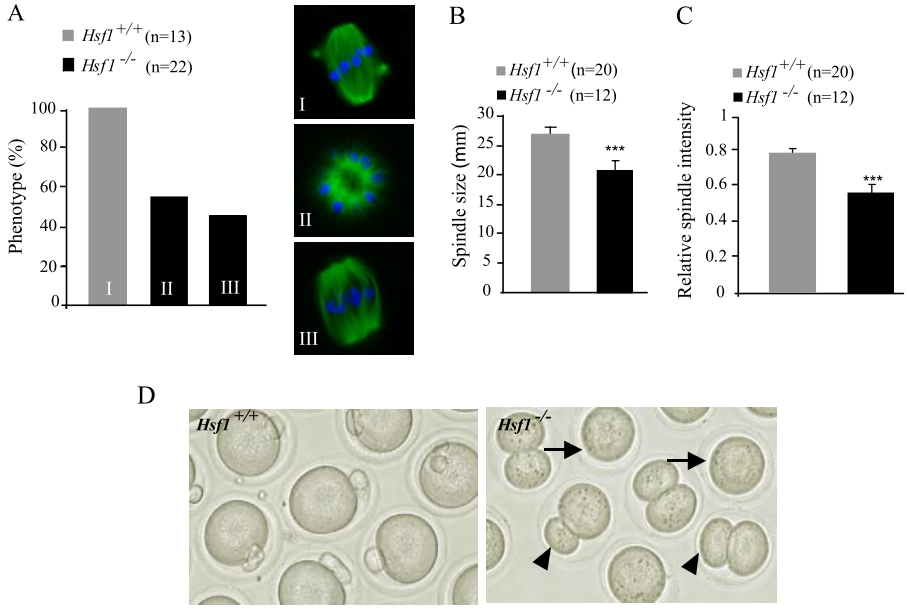

FIGURE 4. **Abnormal spindle and cytokinesis in *Hsf1*$^{-/-}$ oocytes.** *A*, a representative picture and the percentage of cells displaying the corresponding morphology are shown for *Hsf1*$^{+/+}$ and *Hsf1*$^{-/-}$ oocytes. Immunostaining was performed at 10 h for *Hsf1*$^{+/+}$ oocytes to analyze them before they reached meiotic cytokinesis and at 14 h for *Hsf1*$^{-/-}$ oocytes to take into account their GVBD delay. *B*, the length of bipolar spindles was evaluated and plotted for *Hsf1*$^{+/+}$ and *Hsf1*$^{-/-}$ oocytes. *C*, maximal level of microtubular spindle intensity was measured and plotted for *Hsf1*$^{+/+}$ and *Hsf1*$^{-/-}$ oocytes. *B* and *C*, means ± S.E. ***, $p < 0.001$. *D*, representative picture of *Hsf1*$^{+/+}$ and *Hsf1*$^{-/-}$ oocytes after 16 h of culture. *Hsf1*$^{+/+}$ oocytes show the first polar body, indicating that they had reached MII (*left panel*). *Hsf1*$^{-/-}$ oocytes are either blocked after GVBD (*arrows*) or have completed maturation but frequently exhibit larger polar bodies (*arrowheads*).

Hsf1$^{-/-}$ oocytes reached MII (Fig. 3*C*), in comparison to 54.6% of *Hsf1*$^{+/+}$ oocytes ($n = 214/393$). We retrospectively measured the duration of meiotic maturation in *Hsf1*$^{-/-}$ oocytes, which had reached the MII. Although they were all retarded for GVBD, they took the same time as *Hsf1*$^{+/+}$ oocytes to progress from GVBD to MII (Fig. 3*D*).

To better assess meiotic arrest in *Hsf1*$^{-/-}$ oocytes, we analyzed spindle morphology by immunostaining with anti-tubulin antibodies. Normally, the meiotic spindle progresses from a ball of microtubules to a bipolar structure (Figs. 3*A* and 4, *A*, *I*). At 14 h we observed two categories of *Hsf1*$^{-/-}$ oocytes (Fig. 4*A*, *II* and *III*, and supplemental Fig. S2). Representative examples of the first category are shown in Fig. 4*A*, *II*); these *Hsf1*$^{-/-}$ oocytes still exhibited a microtubular ball, indicating that they had failed to organize a bipolar spindle, and consequently, they did not achieve the first meiotic division. The second category corresponds to *Hsf1*$^{-/-}$ oocytes that had built a bipolar spindle (Fig. 4*A*, *III*) but which remained shorter and displayed a reduced microtubular density in comparison to *Hsf1*$^{+/+}$ spindles (Fig. 4, *B* and *C*).

Finally, oocyte maturation ends with the first meiotic division, resulting in the extrusion of the first polar body, which contains less than 20% of the oocyte volume. Hence, in contrast to most somatic cell divisions, meiotic cytokinesis is strongly asymmetrical. This characteristic was lost in a significant proportion of *Hsf1*$^{-/-}$ oocytes that had undergone the first meiotic division to produce an enlarged polar body or had even divided symmetrically (Fig. 4*D* and see Fig. 6*A*).

From these data we conclude that meiosis in *Hsf1*$^{-/-}$ oocytes is severely affected, and we sought to test the hypothesis that this meiotic syndrome (GVBD delay, pro MI arrest, abnormal cytokinesis) is linked to the deficiency in Hsp90α expression we had identified.

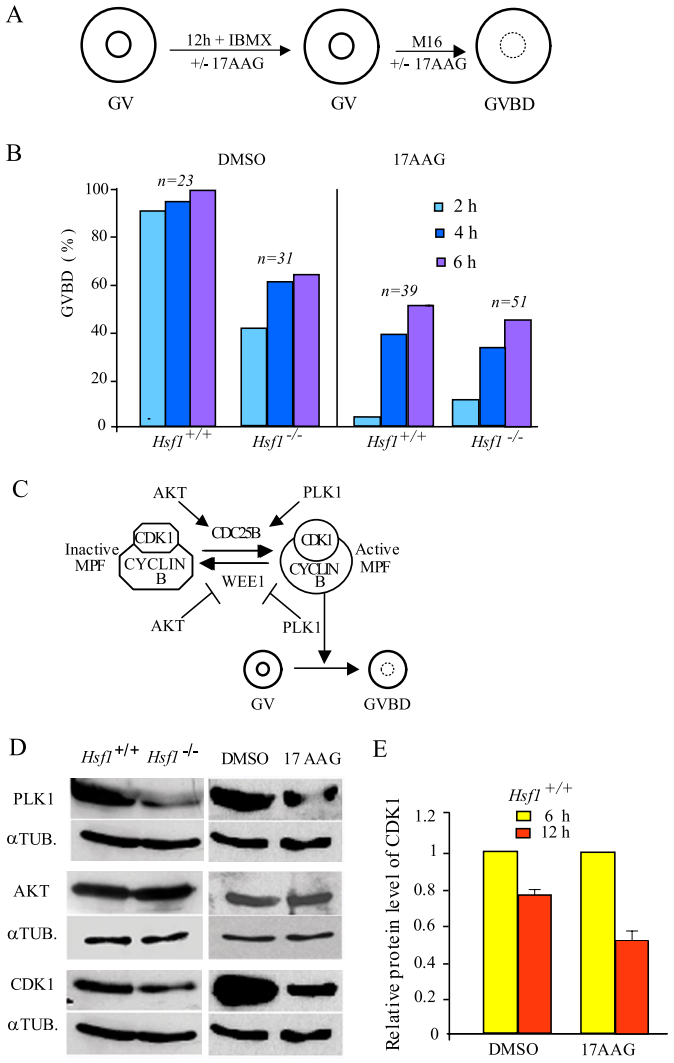

FIGURE 5. **GVBD or G_2/M timing and regulation in *Hsf1*$^{-/-}$- and 17AAG-treated oocytes.** *A*, experimental procedure used to preincubate and culture GV oocytes with 17AAG. IBMX was added to M16 medium to maintain oocytes at GV stage during 17AAG preincubation. *B*, GVBD rate measured at 2, 4, and 6 h after IBMX release to allow meiosis resumption. Numbers of oocytes are as indicated. *C*, simplified model for the regulation of G_2/M transition or meiosis resumption; PLK1 and AKT act upstream of CDK1 by either inhibiting WEE1 or by allowing CDC25B activity to subsequently induce active cyclin B-CDK1/maturation promoting factor (*MPF*) and G_2/M transition (36). *D*, *left panels* present immunoblots prepared with *Hsf1*$^{+/+}$ or *Hsf1*$^{-/-}$ oocyte extract (n = 80 per lane). *Right panels* show immunoblots prepared with oocyte extract (n = 100 per lane) obtained after 12 h of incubation in medium supplemented with IBMX and DMSO or 17AAG. Membranes were probed with PLK1, CDK1, and AKT antibodies as indicated and reprobed with anti-tubulin α (*αTUB.*) as loading control. *E*, histograms represent the relative level of CDK1 in oocytes cultured in the presence of DMSO or 17AAG and treated with cycloheximide for 6 h (*yellow bars*) or 12 h (*red bars*). The CDK1 level evaluated at 6 h of culture was normalized to 1. Data are the means ± S.E.

Timing of Meiotic Resumption (G_2/M) Is under HSF1-Hsp90 Control—G_2/M transition occurs spontaneously and rapidly after isolation of the oocytes from their ovarian follicles. To determine the role of HSF1-Hsp90 in this initial step of meiotic maturation, we compared *Hsf1*$^{-/-}$ with wild-type oocytes treated or not with 17AAG, a specific inhibitor of Hsp90 (26). Because the inhibitory action of 17AAG requires several hours, as shown in cancer cells (21), we preincubated fully grown oocytes for 12 h with the drug in IBMX medium to prevent resumption of meiosis. After removal of IBMX (t = 0 h), we scored GVBD at 2, 4, and 6 h (Fig. 5*A*).

Within 2 h GVBD had occurred in 91% of untreated and in 3% of 17AAG-treated oocytes (Fig. 5*B*). At 6 h, about half of the 17AAG-treated oocytes had resumed meiosis, indicating they had been delayed for several hours in comparison to untreated oocytes. This delay was more severe than in *Hsf1*$^{-/-}$ oocytes probably due to the fact that the inhibitor abolished Hsp90 function completely, whereas HSF1 deficiency only reduced it. Because we observed the same delay in *Hsf1*$^{-/-}$ as in *Hsf1*$^{+/+}$ oocytes when they were treated with 17AAG, we conclude that GVBD is dependent on Hsp90 function (Fig. 5*B*). In addition, we observed that treated *Hsf1*$^{+/+}$ oocytes that had not undergone G_2/M by 6 h could not resume meiosis and remained at the GV stage. This further suggests the importance of Hsp90 activity in meiosis resumption.

GVBD or meiotic G_2/M transition depends on a complex network of kinases and phosphatases that regulates maturation promoting factor (*MPF*) activity (Fig. 5*C*). Several kinases, such as PLK1, AKT, and CDK1, involved in the control of GVBD, are also Hsp90 clients, which means that these proteins transiently interact with Hsp90, thus becoming stabilized and acquiring their proper active conformation. Thus, in the absence of adequate Hsp90 activity, these proteins should be prone to degradation. We analyzed the levels of PLK1, AKT, and CDK1 by Western blots in both *Hsf1*$^{-/-}$ and 17AAG-treated Hsf1$^{+/+}$ oocytes. PLK1 and CDK1 levels were clearly reduced, whereas the amount of AKT was unchanged (Fig. 5*D*).

To further demonstrate that Hsp90 activity is important in preventing client degradation, we determined the stability of PLK1 and CDK1 in oocytes cultured as before with or without 17AAG and maintained under translation inhibition by cycloheximide for 6 and 12 h in culture. When we compared the amounts of PLK1 and CDK1 at these two time points, we could not detect significant changes for PLK1 (data not shown), but we observed that the CDK1 level was markedly reduced between 6 and 12 h of culture (Fig. 5*E*). Taken together, these data suggested that the GVBD is delayed both in Hsp90-depleted and Hsp90-inhibited oocytes because more time is required for accumulation of the amount of CDK1-cyclin B complex needed for maturation promoting factor activity to reach the threshold level necessary to reinitiate meiosis.

Defective Asymmetrical Division in Maturing Oocytes Treated with 17AAG—To further test the effects of Hsp90 inhibition on meiosis progression and because long exposure to 17AAG partially prevented meiosis resumption, we collected and directly treated maturing oocytes. Under these conditions, the same percentage of MII was obtained in treated and non-treated oocytes. Nevertheless, we observed a significant number of cases of abnormal cytokinesis in 17AAG-treated oocytes, which produced larger polar bodies (77% for treated *versus* 4.5% for untreated *Hsf1*$^{+/+}$ oocytes; Fig. 6*A*). This phenotype was strongly reminiscent of that we had noticed in 28% *Hsf1*$^{-/-}$ oocytes (Fig. 4*D*).

Meiotic cytokinesis is normally delayed until the spindle has migrated to occupy a cortical position (see the diagram in Fig. 6*B*). One explanation of the formation of large polar bodies is that cytokinesis is deregulated and occurs too early before the

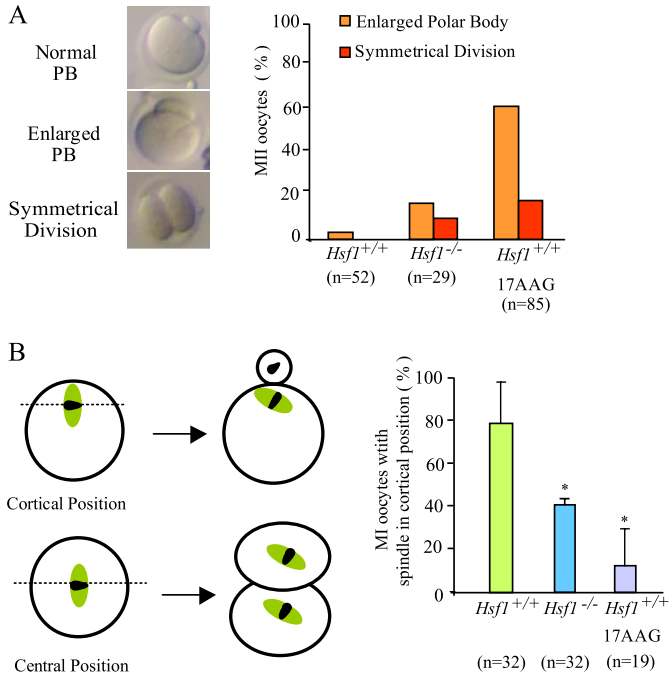

FIGURE 6. **Abnormal cytokinesis and spindle mispositioning in *Hsf1*$^{-/-}$- and 17AAG-treated oocytes.** *A*, representative pictures of the different categories of MII oocytes after extrusion of either normal polar body (*Normal PB*), polar body representing more than 20% of the oocyte volume (*enlarged PB*), or symmetrical division. Percentages of abnormal PB are shown for *Hsf1*$^{+/+}$, *Hsf1*$^{-/-}$, and 17AAG-treated oocytes. *B*, position of the spindle in *Hsf1*$^{-/-}$ and 17AAG-treated *Hsf1*$^{+/+}$ oocytes. Numbers of oocytes (*n*) are as indicated. Data are the means ± S.E.; *, $p < 0.05$.

spindle has normally reached the cortex. This was observed, for example, in oocytes deficient in MAD2, an important regulator of the spindle assembly checkpoint (27). However, this was not the case for *Hsf1*$^{-/-}$ or 17AAG-treated *Hsf1*$^{+/+}$ oocytes, as the extrusion of the first polar body was not accelerated (Fig. 3*D*, supplemental Table S3). Thus, the defect could reside in the migration of the bipolar spindle itself in *Hsf1*$^{-/-}$ and 17AAG-treated oocytes. This was confirmed by the significantly lower frequency of spindles located near the cortex in the maturing oocytes (Fig. 6*B*).

Reduced Activity of the MAP Kinase Pathway in Maturing Hsf1$^{-/-}$ *Oocytes*—At the molecular level, the MAP kinase (MAPK) pathway (Mos → MEK → ERK1/2) was shown to regulate the asymmetry of the first meiotic division. For example, genetic inactivation of *Mos* or depletion of MEK1 in mouse oocytes significantly increased the frequency of extrusion of a large polar body (28, 29). Therefore, we explored the hypothesis that reduced MAPK activity is the reason for the higher incidence of large polar bodies in oocytes lacking HSF1 and full activity of Hsp90. We consequently followed MAPK activity by immunodetection of the phosphorylated form of ERK1/2, the downstream target of MEK1. According to the literature, MAPK activity increases rapidly from 1 to 3 h post-GVBD and then remains stable until the end of maturation (30). Taking into account the observation that *Hsf1*$^{-/-}$ oocytes exhibit variable delays and block in meiosis progression, whereas 17AAG-treated oocytes are able to reach the MII stage, we first examined the level of ERK1/2-P by immunofluorescence (Fig. 7*A*). We selected the oocytes that exhibited a metaphase I plate and a bipolar spindle, indicating that they would probably undergo cytokinesis. Image analysis revealed that the relative amount of ERK1/2-P was lower in *Hsf1*$^{-/-}$ than in *Hsf1*$^{+/+}$ oocytes (Fig. 7, *B* and *C*). Then we collected *Hsf1*$^{-/-}$ and 17AAG-treated oocytes after 14 h of culture and performed Western blots. Fig. 7*D* shows a representative example, indicating that the level of ERK1/2-P was decreased in those oocytes in comparison to *Hsf1*$^{+/+}$ oocytes. Taken together, our morphological and molecular data indicate that Hsp90 activity is required to achieve normal, *i.e.* asymmetrical, oocyte meiosis I and suggest that this may occur through the regulation of the MAP kinase pathway.

DISCUSSION

Mammalian oocytes are highly specialized cells engaged in a complex meiotic cell division, characterized by several "stops and starts" preceding the formation of the zygote through spermatozoon fusion and fertilization (Fig. 3*A*) (31). Once oocytes resume meiosis, they rely on maternal factors stored during oogenesis to sustain the subsequent developmental steps until the maternal-to-zygotic transition occurs (32, 33). We previously reported that HSF1 is one of the few maternal factors in mammals required for female reproductive success (12). In that paper we mainly focused our attention on post-mating events and concluded that *Hsf1* loss of function prevented *Hsf1*$^{-/-}$ females from producing viable embryos, as they were all arrested before the blastocyst stage. To better understand such a maternal effect mutation from a developmental point of view, it is crucial to analyze molecular and cellular events carefully, starting with the oocyte itself. This was the purpose of the present study, and unexpectedly, we found that HSF1 plays a critical part in the regulation of oocyte meiosis and that this can be linked to its transcriptional regulation of Hsp90α, the prominent chaperone expressed in oocytes.

From the evolutionary point of view, Hsp90 was previously shown to play a role in the meiotic maturation of *Caenorhabditis elegans* and *Xenopus laevis* oocytes, but no link was made with HSF1 in these studies (34, 35). Furthermore, Hsp90 activity operated differently in the regulation of meiosis in these organisms (34, 35). The nematode *C. elegans* uses the Daf-21/Hsp90 homolog to ensure the normal function of Wee (WEE-1.3), which is responsible for diakinesis arrest. Consequently, siRNA-mediated Daf-21 loss of function led to aberrant cell cycle progression and endomitotic oocytes (34). In lower vertebrates such as *X. laevis*, Hsp90 is instrumental in activating the Mos kinase that is essential to induce oocyte maturation in amphibians but not in mammals (35). Taken together with these data, our results indicate that the involvement of Hsp90 in oocyte maturation is conserved through evolution, but the key Hsp90 clients appear to be different according to the species and to species-related regulation of oocyte maturation (36).

It is interesting to note that, whereas there is only one Hsp90 gene in lower species, mammals evolved with two cytoplasmic Hsp90 isoforms, Hsp90α and -β, both reported to be regulated by HSF1 (8). Strikingly, oocytes contain almost exclusively the Hsp90α isoform and do not compensate with Hsp90β for Hsp90α down-regulation in the absence of HSF1. Although numerous studies did not distinguish between these two cyto-

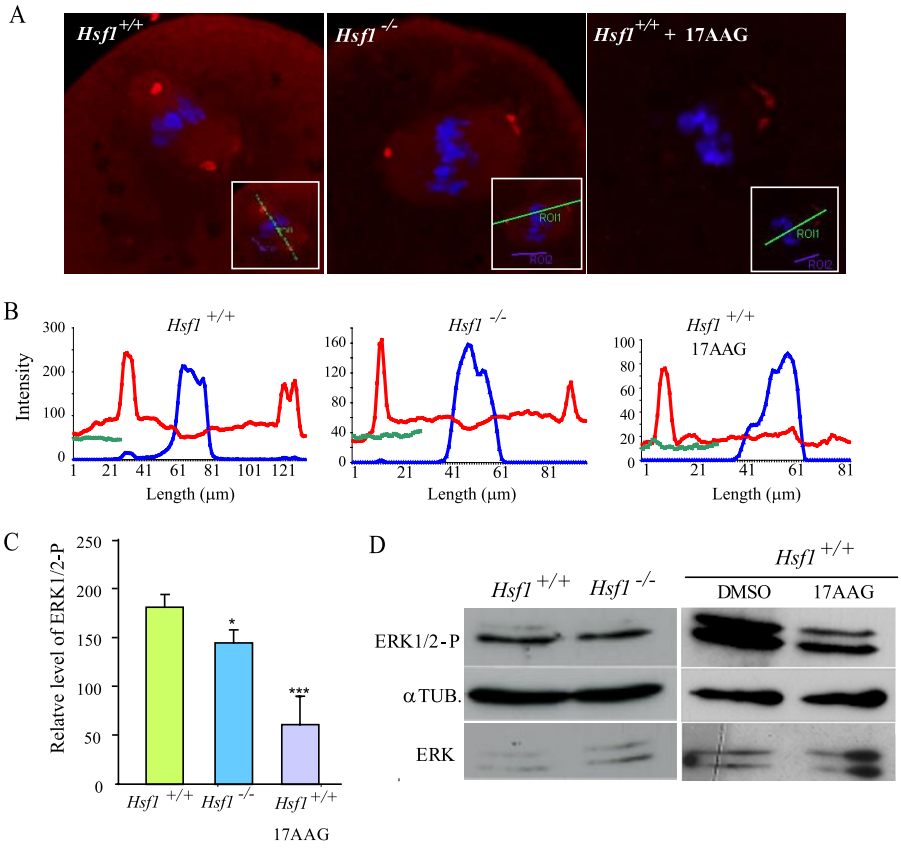

FIGURE 7. **MAPK pathway activity in *Hsf1*$^{-/-}$- and 17AAG-treated oocytes.** *A*, metaphase I oocytes were immunostained for ERK1/2-P and labeled with TO-PRO 3 to visualize the chromosomes. GVBD oocytes were collected at 10 h for untreated and 17AAG-treated *Hsf1*$^{+/+}$ and at 14 h after IBMX release for *Hsf1*$^{-/-}$ oocytes to take into account their GVBD delay. *Insets* show the *bars* drawn along the longest spindle axis used for quantification (*B*). *B*, intensity of the fluorescent signals was measured along the spindle axis (*x* axis, μm) and shown for ERK1/2-P (*red curve*), TO-PRO 3 (*blue curve*), and background (*green curve*). *C*, relative level of ERK1/2-P signal was calculated using the data presented in *B*, and the background value (*green curve*) was subtracted from the peak value of ERK1/2-P signal (*red curve*). Data are the mean ± S.E. *, $p < 0.05$; ***, $p < 0.001$. *D*, Western blots for ERK1/2-P were performed using total protein extracts from *Hsf1*$^{+/+}$, *Hsf1*$^{-/-}$, and 17AAG-treated oocytes isolated and cultured for 12 h ($n = 80$). Tubulin (*αTUB.*) was used as the loading control.

plasmic Hsp90 isoforms, which are highly homologous, our data demonstrate that these two genes are independently regulated and acquire specialized functions in specific cell types (this paper and Voss *et al.* Ref. 18).

The meiotic syndrome described in the present paper (delayed G_2/M transition, partial GVBD block, and defective asymmetrical division) has not been reported previously. With respect to the G_2/M transition, CDK1, which was reported to be a critical limiting factor in female gametes (37), was significantly diminished in *Hsf1*$^{-/-}$ and 17AAG-treated oocytes. Thus, our work appears to be in agreement with data collected from several cell lines in which Hsp90 inhibition was found to perturb G_2/M transition and reduce CDK1 stability through increased proteasomal degradation (21, 38–40).

At a moment when maturing oocytes contained a bipolar spindle, most HSF1-deficient oocytes exhibited a wide range of abnormal microtubular structures. In half of them we noted a typical form which was described elsewhere as a "microtubular ball," indicating an early blockage in pro-metaphase I (41). Such a phenotype was observed in oocytes treated with monastrol, an inhibitor of the kinesin, Eg5 (41), or with double-stranded RNA against cdc6 (42). So far there is no evidence of any link between these genes and *Hsf1*. In contrast, more is known about the role of Hsp90 and microtubule stabilization (21, 43). Thus, deficient spindle organization could be because of severe disturbance of meiotic regulation in addition to defaults in microtubular assembly. Although more work is needed to understand this cellular anomaly better, it is likely to be responsible for meiotic arrest in *Hsf1*$^{-/-}$ oocytes. This leads to a dramatically small number of *Hsf1*$^{-/-}$ oocytes reaching the MII stage required for normal fertilization and development.

The last, but significant, defect concerns the asymmetrical cytokinesis. It is important for oocytes to retain most of the maternal factors stored during oogenesis to sustain future embryonic development. Small polar bodies are extruded because before the division the meiotic spindle migrated from a central position to the cortex thanks to the actin cytoskeleton. Lack of spindle migration and formation of large polar bodies can be observed under several circumstances such as heat shock or brefeldin treatment, MAD2 depletion, and deficiency in the MAP kinase pathway (27, 28, 44). Based on cytokinesis timing, we could rule out a primary defect in spindle checkpoint. In contrast, the level of ERK1/2-P, interpreted as an indication of MAPK pathway activity, was clearly reduced in *Hsf1*$^{-/-}$ oocytes. Our experiments show that, again, Hsp90 is required to sustain MAPK activity in oocytes.

Although our data clearly demonstrate that the activity of the HSF1-dependent Hsp90 is required for mouse oocyte meiosis, we cannot rule out that other HSF1 target genes contribute to the pleiotropic meiotic phenotype described in this paper and/or to the early embryonic death previously reported (12). We are currently working to identify and characterize plausible candidates.

Acknowledgments—We are particularly grateful to C. Charry for genotyping Hsf1 knock-out mice. We thank A. Conter for immunohistochemistry and I. J. Benjamin, B. Ducommun, R. Morimoto, and our colleagues from the Centre de Biologie du Développement for generous gift of reagents and helpful discussion. We acknowledge the use of the imaging facilities (CBD-IFR109) and B. Ronsin for help with movie files. We are indebted to J. Smith for a critical review of the content and the English of the manuscript.

REFERENCES

1. Pirkkala, L., Nykanen, P., and Sistonen, L. (2001) *FASEB J.* **15,** 1118–1131
2. Christians, E. S., and Benjamin, I. J. (2006) *Handb. Exp. Pharmacol.* 139–152
3. Xiao, X., Zuo, X., Davis, A. A., McMillan, D. R., Curry, B. B., Richardson, J. A., and Benjamin, I. J. (1999) *EMBO J.* **18,** 5943–5952
4. Zhang, Y., Huang, L., Zhang, J., Moskophidis, D., and Mivechi, N. (2002) *J. Cell. Biochem.* **86,** 376–393
5. Inouye, S., Izu, H., Takaki, E., Suzuki, H., Shirai, M., Yokota, Y., Ichikawa, H., Fujimoto, M., and Nakai, A. (2004) *J. Biol. Chem.* **279,** 38701–38709
6. Yan, L. J., Christians, E. S., Liu, L., Xiao, X., Sohal, R. S., and Benjamin, I. J. (2002) *EMBO J.* **21,** 5164–5172
7. Zheng, H., and Li, Z. (2004) *J. Immunol.* **173,** 5929–5933
8. Trinklein, N. D., Murray, J. I., Hartman, S. J., Botstein, D., and Myers, R. M. (2004) *Mol. Biol. Cell* **15,** 1254–1261
9. Takaki, E., Fujimoto, M., Sugahara, K., Nakahari, T., Yonemura, S., Tanaka, Y., Hayashida, N., Inouye, S., Takemoto, T., Yamashita, H., and Nakai, A. (2006) *J. Biol. Chem.* **281,** 4931–4937
10. Fujimoto, M., Izu, H., Seki, K., Fukuda, K., Nishida, T., Yamada, S., Kato, K., Yonemura, S., Inouye, S., and Nakai, A. (2004) *EMBO J.* **23,** 4297–4306
11. Dai, C., Whitesell, L., Rogers, A. B., and Lindquist, S. (2007) *Cell* **130,** 1005–1018
12. Christians, E., Davis, A. A., Thomas, S. D., and Benjamin, I. J. (2000) *Nature* **407,** 693–694
13. Vitale, A. M., Calvert, M. E., Mallavarapu, M., Yurttas, P., Perlin, J., Herr, J., and Coonrod, S. (2007) *Mol. Reprod. Dev.* **74,** 608–616
14. Kregel, K. C. (2002) *J. Appl. Physiol.* **92,** 2177–2186
15. Huang, L., Min, J. N., Masters, S., Mivechi, N. F., and Moskophidis, D. (2007) *Genesis* **45,** 487–501
16. Huang, L., Mivechi, N. F., and Moskophidis, D. (2001) *Mol. Cell. Biol.* **21,** 8575–8591
17. Hunt, C. R., Dix, D. J., Sharma, G. G., Pandita, R. K., Gupta, A., Funk, M., and Pandita, T. K. (2004) *Mol. Cell. Biol.* **24,** 899–911
18. Voss, A. K., Thomas, T., and Gruss, P. (2000) *Development* **127,** 1–11
19. McMillan, D. R., Xiao, X., Shao, L., Graves, K., and Benjamin, I. J. (1998) *J. Biol. Chem.* **273,** 7523–7528
20. Van Cauwenberge, A., and Alexandre, H. (2000) *Int. J. Dev. Biol.* **44,** 409–420
21. de Carcer, G. (2004) *Cancer Res.* **64,** 5106–5112
22. Livak, K. J., and Schmittgen, T. D. (2001) *Methods* **25,** 402–408
23. Chang, Y., Ostling, P., Akerfelt, M., Trouillet, D., Rallu, M., Gitton, Y., El Fatimy, R., Fardeau, V., Le Crom, S., Morange, M., Sistonen, L., and Mezger, V. (2006) *Genes Dev.* **20,** 836–847
24. Laemmli, U. K. (1970) *Nature* **227,** 680–685
25. Salmand, P. A., Jungas, T., Fernandez, M., Conter, A., and Christians, E. S. (2008) *Biol. Reprod.* **79,** 1092–1101.
26. Whitesell, L., and Lindquist, S. L. (2005) *Nat. Rev. Cancer* **5,** 761–772
27. Homer, H. A., McDougall, A., Levasseur, M., Yallop, K., Murdoch, A. P., and Herbert, M. (2005) *Genes Dev.* **19,** 202–207
28. Choi, T., Fukasawa, K., Zhou, R., Tessarollo, L., Borror, K., Resau, J., and Vande Woude, G. F. (1996) *Proc. Natl. Acad. Sci. U. S. A.* **93,** 7032–7035
29. Yu, L. Z., Xiong, B., Gao, W. X., Wang, C. M., Zhong, Z. S., Huo, L. J., Wang, Q., Hou, Y., Liu, K., Liu, X. J., Schatten, H., Chen, D. Y., and Sun, Q. Y. (2007) *Cell Cycle* **6,** 330–338
30. Verlhac, M. H., Kubiak, J. Z., Clarke, H. J., and Maro, B. (1994) *Development* **120,** 1017–1025
31. Mehlmann, L. M. (2005) *Reproduction* **130,** 791–799
32. Schultz, R. M. (2002) *Hum. Reprod. Update* **8,** 323–331
33. Hamatani, T., Yamada, M., Akutsu, H., Kuji, N., Mochimaru, Y., Takano, M., Toyoda, M., Miyado, K., Umezawa, A., and Yoshimura, Y. (2008) *Reproduction* **135,** 581–592
34. Inoue, T., Hirata, K., Kuwana, Y., Fujita, M., Miwa, J., Roy, R., and Yamaguchi, Y. (2006) *Dev. Growth Differ* **48,** 25–32
35. Fisher, D. L., Mandart, E., and Doree, M. (2000) *EMBO J.* **19,** 1516–1524
36. Han, S. J., and Conti, M. (2006) *Cell Cycle* **5,** 227–231
37. Kanatsu-Shinohara, M., Schultz, R. M., and Kopf, G. S. (2000) *Biol. Reprod.* **63,** 1610–1616
38. Garcia-Morales, P., Carrasco-Garcia, E., Ruiz-Rico, P., Martinez-Mira, R., Menendez-Gutierrez, M. P., Ferragut, J. A., Saceda, M., and Martinez-Lacaci, I. (2007) *Oncogene* **26,** 7185–7193
39. Nomura, N., Nomura, M., Newcomb, E. W., and Zagzag, D. (2007) *Biochem. Pharmacol.* **73,** 1528–1536
40. Nakai, A., and Ishikawa, T. (2001) *EMBO J.* **20,** 2885–2895
41. Schuh, M., and Ellenberg, J. (2007) *Cell* **130,** 484–498
42. Anger, M., Stein, P., and Schultz, R. M. (2005) *Biol. Reprod.* **72,** 188–194
43. Takaki, E., Fujimoto, M., Nakahari, T., Yonemura, S., Miyata, Y., Hayashida, N., Yamamoto, K., Vallee, R. B., Mikuriya, T., Sugahara, K., Yamashita, H., Inouye, S., and Nakai, A. (2007) *J. Biol. Chem.* **282,** 37285–37292
44. Wang, L., Wang, Z. B., Zhang, X., FitzHarris, G., Baltz, J. M., Sun, Q. Y., and Liu, X. J. (2008) *Dev. Biol.* **313,** 155–166
45. Dale, E. C., Yang, X., Moore, S. K., and Shyamala, G. (1997) *Cell Stress Chaperones* **2,** 87–93